Geoscience Frontiers 5 (2014) 289–298

Contents lists available at SciVerse ScienceDirect

China University of Geosciences (Beijing)

Geoscience Frontiers

journal homepage: www.elsevier.com/locate/gsf

Research paper

Type division and controlling factor analysis of 3rd-order sequences in marine carbonate rocks

Yunbo Zhang [a,*], Zongju Zhao [b], Genhou Wang [a], Zaixing Jiang [a], Mingjian Wang [c], Min Zheng [d], Shiben Zhang [d]

[a] China University of Geosciences (Beijing), Beijing 100083, China
[b] Chinese Petroleum Society, Beijing 100724, China
[c] Qingdao Institute of Marine Geology, Shandong 266071, China
[d] Research Institute of Petroleum Exploration and Development, Beijing 100083, China

ARTICLE INFO

Article history:
Received 23 August 2012
Received in revised form
2 July 2013
Accepted 3 July 2013
Available online 31 July 2013

Keywords:
Carbon isotope
3rd-Order sequence
Milankovitch cycles
Middle Permian strata
Sichuan Basin

ABSTRACT

Type division and controlling factor analysis of 3rd-order sequence are of practical significance to tectonic analysis, sedimentary environment identification, and other geological researches. Based on the comprehensive analysis of carbon and oxygen isotope trends, paleobathymetry and spectral-frequency of representative well logs, 3rd-order sequences can be divided into 3 types: (a) global sea level (GSL) sequence mainly controlled by GSL change; (b) tectonic sequence mainly controlled by regional tectonic activity; and (c) composite sequence jointly controlled by GSL change and regional tectonic activity. This study aims to identify the controlling factors of 3rd-order sequences and to illustrate a new method for classification of 3rd-order sequences of the middle Permian strata in the Sichuan Basin, China. The middle Permian strata in the Sichuan Basin consist of 3 basin-contrastive 3rd-order sequences, i.e., PSQ1, PSQ2 and PSQ3. Of these, PSQ1 is a GSL sequence while PSQ2 and PSQ3 are composite sequences. The results suggest that the depositional environment was stable during the deposition of PSQ1, but was activated by tectonic activity during the deposition of the middle Permian Maokou Formation.

© 2013, China University of Geosciences (Beijing) and Peking University. Production and hosting by Elsevier B.V. All rights reserved.

1. Introduction

At present, controversy remains over the genesis mechanisms and main controlling factors of 3rd-order sequences. Two major viewpoints are as follows: (a) 3rd-order sequences are primarily controlled by global sea level (GSL) change, thus possessing global comparability (Haq et al., 1987; Haq and Schutter, 2008); and (b) 3rd-order sequences can be controlled by non-global factors, such as regional tectonic activity and isostatic subsidences, thus may not possess global comparability (Duncan et al., 1999; Ward et al., 1999; Abbott and Sweet, 2000; Miall, 2000; Lazauskiene et al., 2003; Horton et al., 2004). In particular, the 3rd-order sequences developed in foreland basins, strike-skip basins, and active rift basins are more frequently controlled by regional tectonic activity (Sabadini et al., 1990; Cathles and Hallam, 1991; Macdonald, 1991; Plint et al., 1992; Miall, 1994).

In the present study, the fundamental reason for disagreement on the existing division of 3rd-order sequence types is related to different sequence developmental characteristics between the glacial and interglacial periods. During the interglacial period, the boundary and cycle characteristics of 4th- (parasequence sets) and 5th-order sequences (parasequences) are not obvious, whereas those of 3rd-order sequences can easily be identified. During the glacial period, the boundary and cycle characteristics of 4th- and 5th-order sequences are distinct, but those of 3rd-order sequences are difficult to be recognized (Ma et al., 1999).

Currently, it remains controversial over the definition of 3rd-order sequence types, primarily due to lack of knowledge regarding their main controlling factors. This issue has become a hot topic in research of sedimentology. In the Permian period, the sedimentary

* Corresponding author. Tel.: +86 10 82322653.
E-mail address: zhangyb@cugb.edu.cn (Y. Zhang).

Peer-review under responsibility of China University of Geosciences (Beijing)

Production and hosting by Elsevier

1674-9871/$ – see front matter © 2013, China University of Geosciences (Beijing) and Peking University. Production and hosting by Elsevier B.V. All rights reserved.
http://dx.doi.org/10.1016/j.gsf.2013.07.002

environment was relatively stable and marine carbonate platform facies were well-developed in the Sichuan Basin. Thus, the Sichuan region provides excellent materials for studying sedimentary sequences in marine carbonate rocks. Taking as an example the middle Permian strata in the Sichuan Basin, this study aims to identify the controlling factors of 3rd-order sequences and to propose a new method for classification of 3rd-order sequences in marine carbonate rocks.

2. Geological setting

The Sichuan Basin (28°N to 32°42′N, 102°30′E to 110°E) is a first-class tectonic unit in the northwestern Yangtze Paraplatform in southwest China. It covers an area of approximate 18×10^4 km^2, with higher terrain in the west and lower terrain in the east. The basin is rhombic-shaped in plane. That is, the slightly longer northwest and southeast boundaries extend along NE direction, whereas the uneven and slightly curved northeast and southwest boundaries extend along NW direction, with little deflection to WE direction (Fig. 1). The four boundaries, which confine the Sichuan Basin, can easily be recognized from the surrounding tectonics.

Previously, a number of studies have been conducted on the sequence stratigraphy of the middle Permian strata in the Sichuan Basin. However, the established 3rd-order sequence divisions are substantially diverse due to various sequence classification criteria and different primary data (e.g., outcrop and seismic data). Several studies divided the middle Permian strata in the Sichuan Basin into seven 3rd-order sequences according to the outcrop data (Qin et al., 1999; Wang et al., 1999; Zhou et al., 2005; Xu et al., 2011), whereas other researchers divided the middle Permian strata into five 3rd-order sequences (Li and Chen, 2008; Wu et al., 2010). As for detailed divisions, there remain significant differences among previous studies mainly because of the obscure boundaries of 3rd-order sequences in the Permian strata of the ice period. The area of cumulative proven natural gas reservoirs is approximate 811.68×10^8 m^3 in the Sichuan Basin (Chen et al., 2007). Therefore, research on sequence stratigraphy of the middle Permian strata in the Sichuan Basin is of great significance to oil-gas exploration and development in marine carbonate rocks.

3. Outcrop sequence characteristics

The Changjianggou outcrop (32°19′29″N, 105°27′2.6″E) is located in the Shangsi village, Guangyuan city in the northwestern Sichuan Basin. Rock samples were collected from the micrite at the base of a meter-scale cyclic sequence. The samples (>5 g each) were ground to powder in the laboratory and then acidified to remove the organic matter content. Only inorganic carbon and oxygen isotopes were retained in samples for further analysis in order to provide data of the GSL change. Detailed measurement and sample analysis of the outcrops show the following characteristics.

3.1. PSQ1

The Liangshan Formation at the base of PSQ1 is approximate 0.82 m thick and mainly consists of claystone and clay shale. The middle Carboniferous Huanglong Formation below the Liangshan Formation is mainly composed of dolostone, with karst caves filled with light-gray, purple and variegated calcite, as well as locally developed crystalline limestone and karst breccias. An obvious unconformity developed between these two formations is recognized as the Type-I sequence boundary. Above the Liangshan Formation,

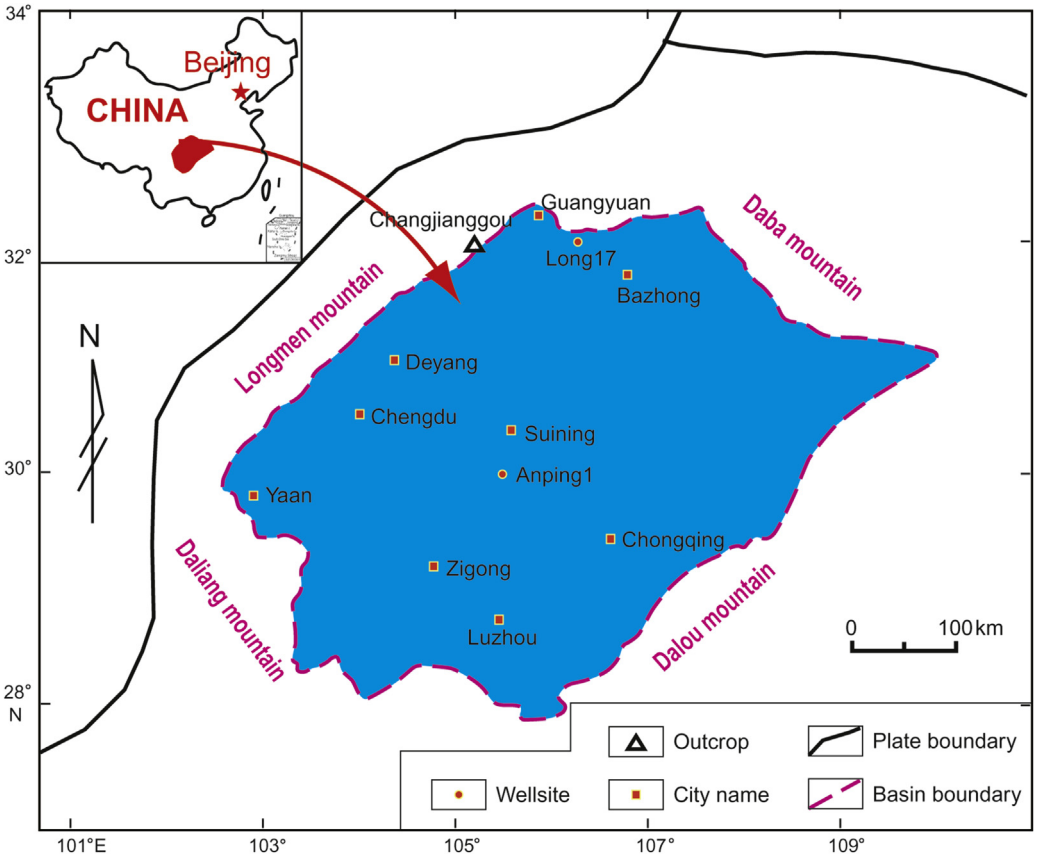

Figure 1. The location of the Sichuan Basin in China.

the Qixia Formation consists of carbonate platform facies sediments deposited in shallow water with shallow to gradually deeper water (Fig. 2a). When paleobathymetry reaches the maximum level, a condensed section is recognized by the occurrence of the 10th layer consisting of irregular, thin-bedded, bioclastic micritic limestone interbedded with black-grey, calcareous mudstone. Therefore, the Liangshan Formation and the 1st–10th layers at the bottom of the Qixia Formation constitute the transgressive systems tract of the first 3rd-order sequence (PSQ1) of the middle Permian strata.

Above the 10th layer of the Qixia Formation, there are multiple upward-shallowing parasequences/parasequence sets (Fig. 2b). The occurrence of such high-frequency cycles reflects the upward-shallowing process of the water depth, and represents the typical highstand systems tract (HST) (Fig. 2b). In particular, the 22nd–25th layers of the upper Qixia Formation consist of grey, thick-bedded, massive sparry calcarenite (Fig. 2c) interbedded by 20 m-thick light-grey, thick-bedded, medium-coarse crystal dolomite, featuring loose lithology and good property. Porphyritic patterns of yellowish-brown dolomite were observed in the 24th layer (Fig. 2d), indicating the formation of platform margin beach subfacies under the high-energy setting and the shallowest sedimentary water condition.

3.2. PSQ2

The Maokou Formation conformably overlies the Qixia Formation. At the base of the Maokou Formation, a suite of dark-grey, thin-medium-bedded, bioclastic micritic limestone interbedded with pelyte forms a lithofacies conversion surface with the top of the underlying Qixia Formation, which is defined as the Type-II sequence boundary (Fig. 3a). In the 33rd layer, grey calcareous mudstone interlayed by a little dark-grey, thin-medium-bedded and partially-lenticular, black-grey, bioclastic micritic limestone represents the maximum flooding surface. These sedimentary rocks form the new condensed section of PSQ2 (Fig. 2b). Across this level, there is a series of upward-shallowing, high-frequency cycles composed of the grey, thin-medium-bedded bioclastic micritic limestone interbedded with grey, medium-thick-bedded, bioclastic micritic limestone, showing typical characteristics of HST (Fig. 3c). As the water becomes shallower, grey, thick-bedded, sparry, calcarenitic and bioclastic limestone appears in the 46th and 47th layers, representing the shallowest water in this section and the development of beach subfacies. This feature also indicates the end of PSQ2 (Fig. 3d).

3.3. PSQ3

In the 48th layer, the presence of a great set of grey, thin-medium-bedded, bioclastic micritic calcarenite reflects the relatively low energy depositional setting. The 47th underlying layer consists of grey, thick-bedded, sparry, calcarenitic and bioclastic micritic limestone. There is a lithology conversation surface developed between the 47th and 48th layers (Fig. 3d). Thus, this

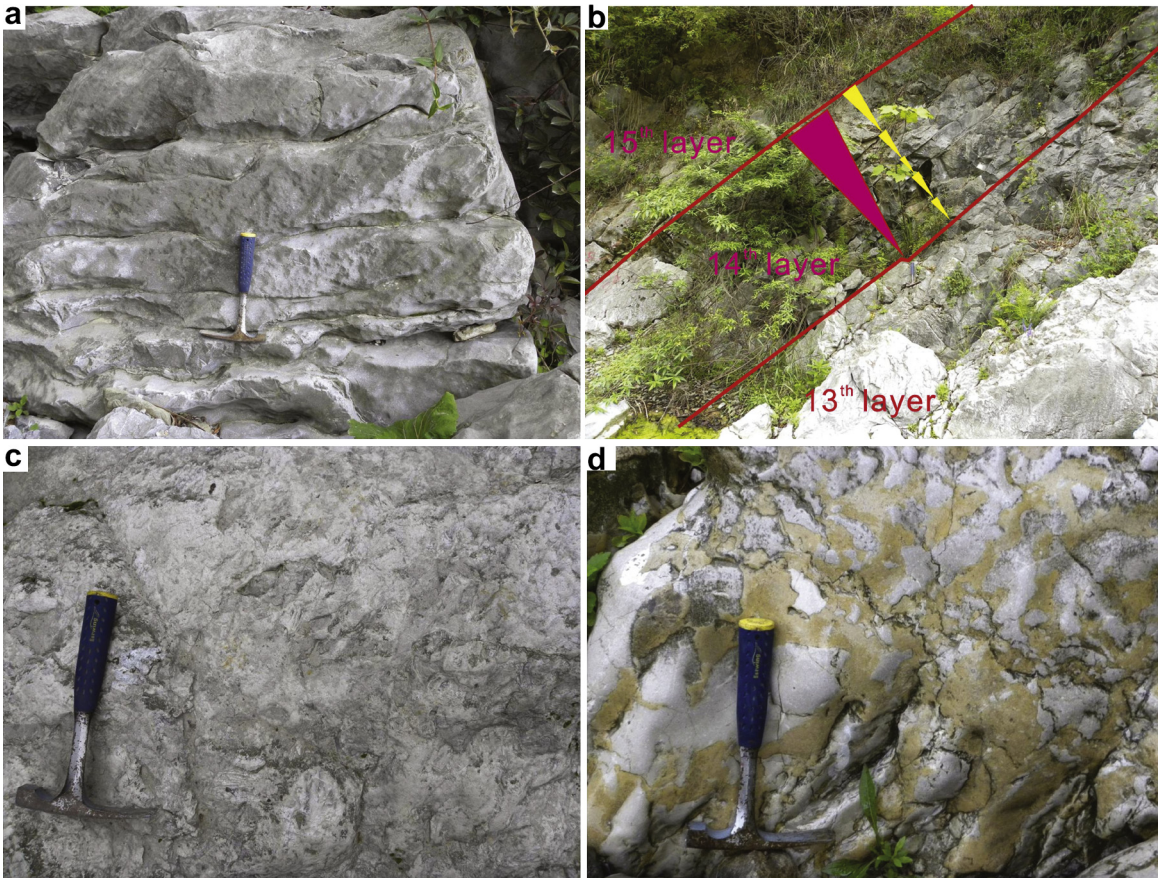

Figure 2. Sedimentary characteristics of the condensed section and high systems tract of the first 3rd-order sequence (PSQ1) at the Changjianggou outcrop. (a) The 10th layer of the Qixia Formation consists of dark-black-grey bioclastic micritic limestone (the condensed section). (b) The parasequences in the high systems tract of PSQ1. The lower part of the 14th layer of the Qixia Formation (three coarsening-upward cycles) is 1.1 m thick and consists of dark-grey, medium-bedded, bioclastic micritic calcarenite. The upper part of 14th layer (one coarsening-upward cycle) is 1.5 m thick and consists of light-grey, thick-bedded, bioclastic micritic dolostone. The four cycles likely represent an upward-shallowing parasequence set of 0.1 million years (parasequence: parasequence set = 1:4). It also shows the characteristics of the high systems tract within the middle ramp subfacies. (c) The top of the 24th layer consists of grey, massive sparry calcarenite. (d) The 22nd layer of the Qixia Formation shows irregular and patchy dolomitization developed among grey, massive sparry calcarenite, with localized coarse-crystal calcareous miarolitic cavity induced by dedolomitization.

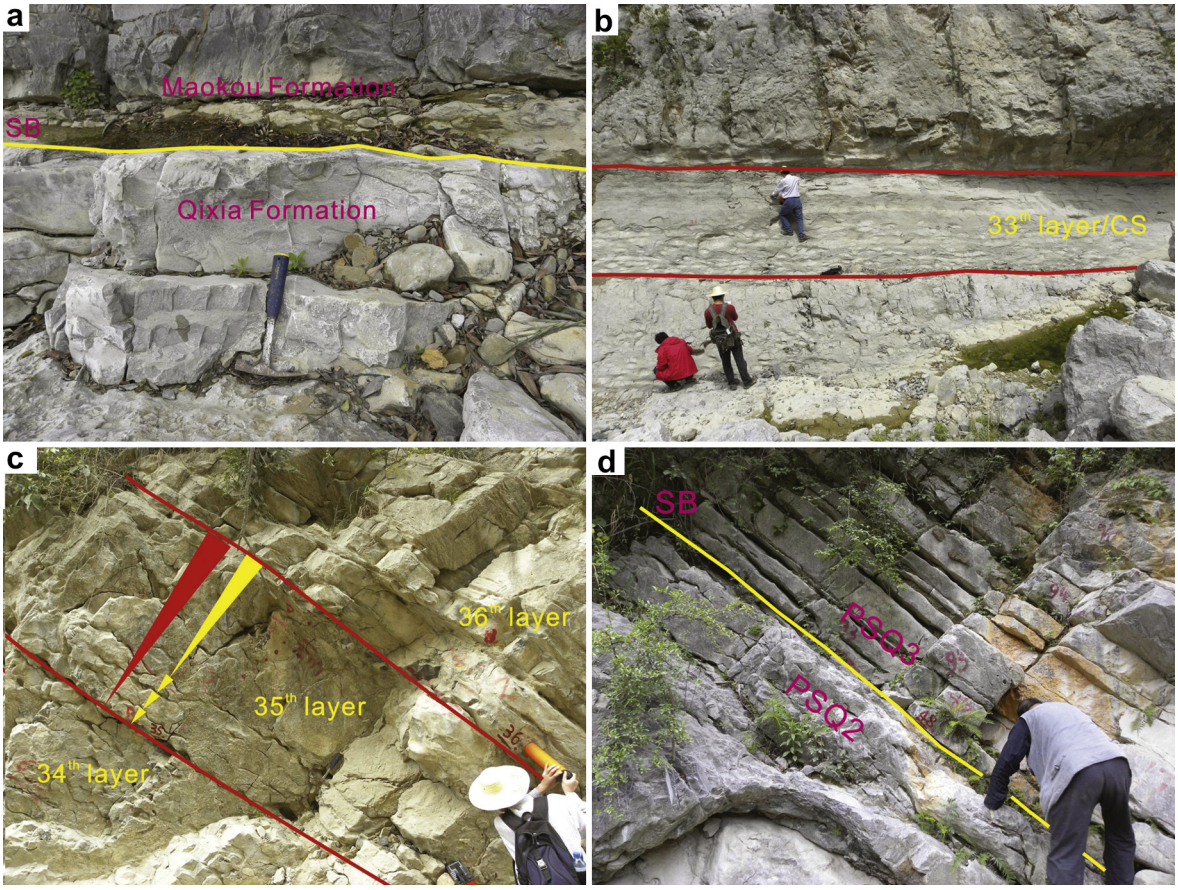

Figure 3. Sedimentary characteristics of the top surface and high systems tract of PSQ2. (a) The sequence boundary (SB) between PSQ1 and PSQ2. The top of the Qixia Formation (below SB) consists of grey, massive, porphyritic, sparry calcarenite undergoing dolomitization, and the base of the Maokou Formation (above SB) consists of dark-grey, medium-bedded, bioclastic micritic limestone and bioclastic micritic limestone interlayed by pelyte. (b) The condensed section of PSQ2. Black-grey, calcareous mudstone interlayed by a little dark-grey, thin-medium-bedded, and locally-lenticular bioclastic micritic limestone. (c) The high systems tract of PSQ2. The 34th–36th layers of the Maokou Formation consist of a series of upward-shallowing high-frequency cycles composed of grey, thin to medium-bedded, bioclastic micritic limestone and grey, medium-thick-bedded, micritic bioclastic limestone. (d) The top boundary of PSQ2. The 47th layer below the sequence boundary within the Maokou Formation consists of grey, thick-bedded, sparry bioclastic micritic calcarenite, and the 48th layer above the sequence boundary in the Maokou Formation consists of thin to medium-bedded, bioclastic micritic limestone.

new sequence is identified as Type-II sequence boundary (Fig. 3d). Upward to the 53rd layer, there is a set of black-grey, calcareous mudstone interbedded with dark-grey, thin-medium-bedded, argillaceous limestone with small amount of locally-developed flint bands and clumps, indicating the condensed section of the new sequence (Fig. 4a). Above the condensed section, multiple upward-shallowing, high-frequency cycles represent the distinct characteristics of HST (Fig. 4b). At the top of the middle Permian strata in the basin, medium-thick-bedded, micritic bioclastic calcarenite appears right below the Wujiaping Formation, indicating the end of the 3rd-order sequence (Fig. 5). There is no obviously exposed karst at the top of the Maokou Formation in this outcrop.

In addition, the natural gamma ray curve as well as the carbon (C) and oxygen (O) isotope curves of the outcrop have an obvious cyclic trend (Fig. 6). The C and O isotope values have distinctly abrupt changes at the interfaces of sequences and systems tracts (Table 1). The lower the water level is, the higher the O isotope values and the lower the C isotope values are, and vice versa (Fig. 6). However, the trend of natural gamma ray curve is not clear. Thus, the middle Permian strata in the Sichuan Basin can be divided into three 3rd-order sequences, i.e., PSQ1, PSQ2 and PSQ3 from bottom to top (Table 2). Of these, PSQ1 corresponds to the Liangshan and Qixia formations, and PSQ2 and PSQ3 correspond to the lower and upper Maokou Formation, respectively. Accordingly, the integrated histogram of the Changjianggou outcrop is plotted (Fig. 6).

4. Drilling sequence characteristics

Paleontological data analysis of outcrops and drillings showed that the middle Permian strata conodont and fusulinid fossils were integrated in the vertical direction and continuously deposited in identified strata of the Sichuan Basin (Zhang et al., 2011). From bottom to top, there are 8 conodont zones, including *Mesogondolella idahoensis*, *Jinogondolella asserata*, *Jinogondolella postserrata*, *Clarkina bitteri-Clarkina liangshanensis* assemble, *Clarkina guangyuanensis*, *Clarkina orientalis*, *Clarkina subcarinata* enrichment *and Clarkina deflecta-Clarkina changxinensis* assemble. Of these, the zones 1–3 and 5–6 are national standard conodont zones in China. In addition, seven fusulinid zones are formed from bottom to top, including *Pseudoschwagerina*, *Misellina*, *Cancellina*, *Neoschwagerina* enrichment, *Yabeina*, *Codonofusiella* and *Palaeofusulina*. The contrast relation between outcrop sequence and drilling-logging sequence was established based on the lithological association and natural gamma ray curves (Fig. 7), and the sedimentary subfacies in the inner, middle and outer ramps were identified in the Sichuan Basin.

The thicknesses of sequences PSQ1 and PSQ2 are uniform across the Sichuan Basin (Fig. 7), suggesting that the sedimentary environment was stable. During this period, the inner ramp sedimentary subfacies widely occurred in the basin, whereas the platform beach subfacies were developed in certain areas (e.g., Gongshen1 and Anping1). There are substantial changes in the thickness of

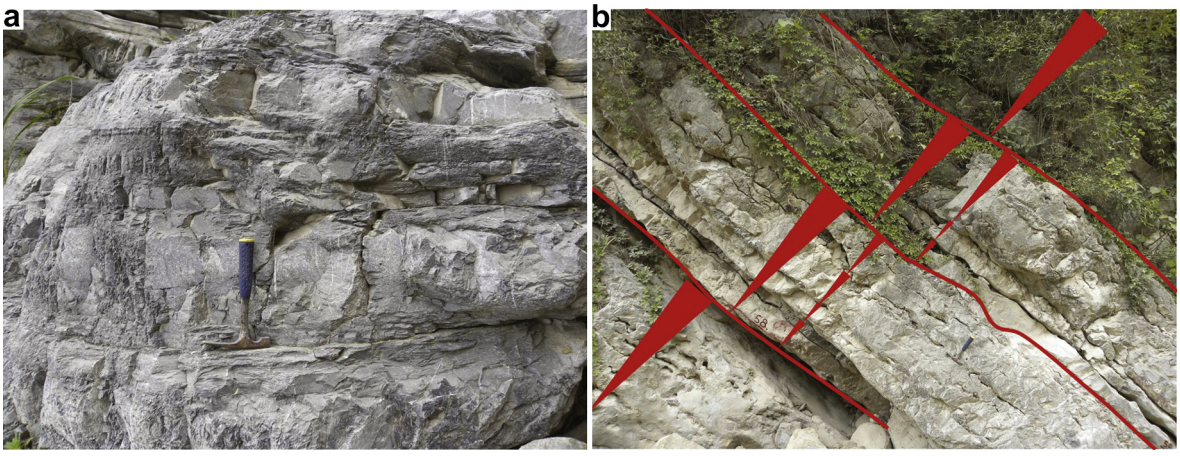

Figure 4. Sedimentary characteristic of the condensed section and high systems tract of PSQ3. (a) The condensed section of PSQ3. Black-grey, calcareous mudstone interbedded with dark-grey, thin-medium-bedded, argillaceous limestone in the 53rd layer of the Maokou Formation. (b) The characteristics of HST of PSQ3. From bottom to top, three upward-shallowing, high-frequency cycles composed of medium-thick-bedded, bioclastic micritic calcarenite in the 58–60th layers.

sequence PSQ3 because of erosion of the upper Maokou Formation. Such changes indicate that the declined tectonic activity significantly affected the deposition of the upper Maokou Formation. In particular, the formation thickness of well Wujia1 significantly changes, and the core appears to be the margin beach subfacies with well-developed strata. These indicate that the sedimentary environment generally shifted from the initial stable state to an activity state in the middle Permian, as confirmed by the C and O isotope variation trends at the Changjianggou outcrop (Fig. 6), as well as associated subfacies change from inner to middle ramp in the northern basin.

5. Sequence types and controlling factors

The middle Permian 3rd-order sequence stratigraphic framework in the Sichuan Basin was established by comprehensive analysis of the sequence characteristics of outcrop, drilling, logging, and the C and O isotope data (Table 1).

5.1. Theoretical principles for sequence classification

Previous studies suggest that relative paleobathymetric changes are mainly controlled by GSL change, tectonic activity, and sedimentary filling rate (Sarg, 1988; Tucker et al., 1990; Macdonald, 1991; Vail et al., 1991; Miall, 2000). It is thought that the sedimentary filling rate is determined by the carbonate production rate, and the latter is mainly controlled by light intensity and paleobathymetry (Wilson, 1975; Schlager, 2005). Thus, carbonate sediment is mainly distributed in the light-saturated zone, ranging from 0 to 20 m and characterized by an exponential decline with increasing paleobathymetry. The production rate of carbonate rock at approximate 100 m paleobathymetric depth is even lower than 10% of that in the light-saturated zone. In addition, the carbonate production decreases with the increasing latitude and is particularly low in high latitude areas, e.g., >30° (Schlager, 2005). The carbonate production rate, as well as tectonic activity and latitude belts within a special plate, would not change much within the

Figure 5. Characteristics of the top surface of sequence PSQ3 and its macroscopic view. The top of the Maokou Formation consists of medium-thick-bedded, bioclastic micritic calcarenite. The base of Wujiaping Formation consists of carbonaceous mudstone, and the Wujiaping Formation mainly consists of thin-medium-bedded micrite interbedded with calcareous mudstone, with hummocky bedding observed in the upper part.

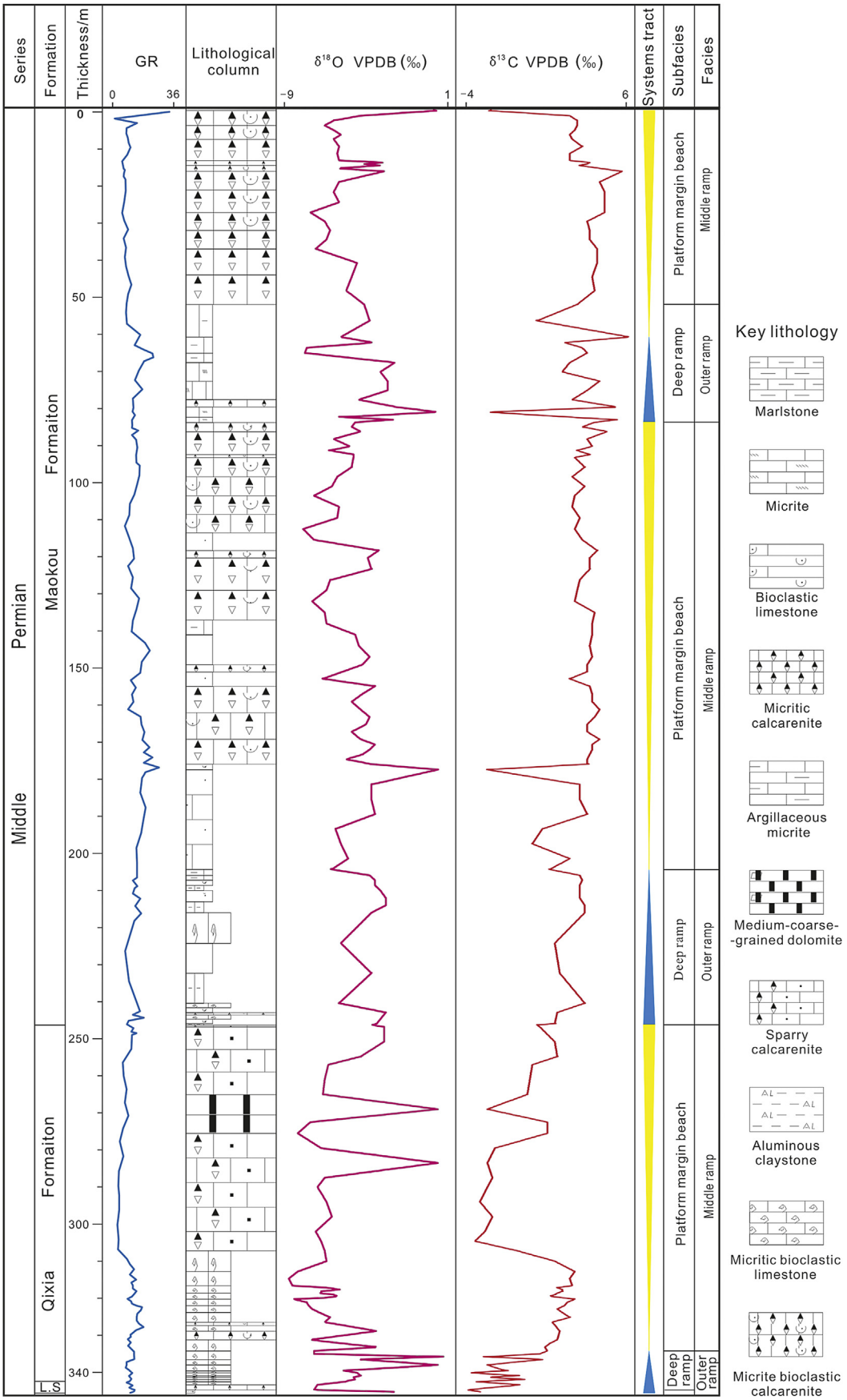

Figure 6. Stratigraphic profile of the Changjianggou outcrop, showing the middle Permian sequences (LS, Liangshan Formation).

Table 1
The C and O isotope values of the samples from the Changjianggou outcrop (Tested in Nanjing University, China).

Sample no.	Sample site (m)	$\delta^{13}C_{VPDB}$ ‰	$\delta^{18}O_{VPDB}$ ‰	Sample no.	Sample site (m)	$\delta^{13}C_{VPDB}$ ‰	$\delta^{18}O_{VPDB}$ ‰	Sample no.	Sample site (m)	$\delta^{13}C_{VPDB}$ ‰	$\delta^{18}O_{VPDB}$ ‰
P2m-T-102	3	3.3	−4.3	P2m-T-51	108	3.4	−5.5	P2q-T-49	245.8	2.1	−3.0
P2m-T-101	4	3.6	−5.8	P2m-T-50	110	3.7	−5.6	P2q-T-48	250	2.7	−3.0
P2m-T-100	5.9	3.6	−6.3	P2m-T-49	113	3.5	−7.5	P2q-T-47	253	2.8	−4.3
P2m-T-99	7	3.5	−5.8	P2m-T-48	116	3.8	−6.9	P2q-T-46	256	1.8	−6.1
P2m-T-98	7.5	3.3	−5.4	P2m-T-47	117.3	4.4	−3.3	P2q-T-45	260	1.7	−6.3
P2m-T-97	9.6	3.4	−5.8	P2m-T-46	119.3	4.1	−3.9	P2q-T-44	264	1.6	−6.4
P2m-T-96	12	3.8	−5.5	P2m-T-45	122	4.1	−3.7	P2q-T-43	269	2.4	−7.1
P2m-T-95	14	3.3	−5.6	P2m-T-44	125.5	3.7	−6.0	P2q-T-42	274.5	2.4	−7.8
P2m-T-94	15.4	3.3	−5.5	P2m-T-43	128	3.6	−6.2	P2q-T-41	280	0.3	−6.5
P2m-T-93	15.8	4.1	−3.0	P2m-T-42	131	3.5	−7.0	P2q-T-40	284	0.2	−6.3
P2m-T-92	16.3	4.0	−4.1	P2m-T-41	134	4.3	−6.3	P2q-T-39	288	0.0	−6.7
P2m-T-91	16.7	3.7	−3.3	P2m-T-40	137	4.2	−6.2	P2q-T-38	292	−0.3	−6.2
P2m-T-90	17.5	4.5	−5.6	P2m-T-39	140	4.2	−4.6	P2q-T-37	297	0.2	−5.9
P2m-T-89	18.3	5.4	−3.0	P2m-T-38	143	4.1	−4.4	P2q-T-36	301	−0.1	−6.8
P2m-T-88	21	4.5	−5.5	P2m-T-37	146	4.2	−3.8	P2q-T-35	303	−0.5	−6.5
P2m-T-87	24	4.7	−5.8	P2m-T-36	148.1	4.0	−4.2	P2q-T-34	306.2	1.2	−6.3
P2m-T-86	27	4.7	−5.5	P2m-T-35	150	4.0	−5.3	P2q-T-33	309	2.7	−6.2
P2m-T-85	29.4	4.7	−7.1	P2m-T-34	152	3.3	−6.4	P2q-T-32	311.8	3.5	−7.8
P2m-T-84	32	4.0	−6.3	P2m-T-33	153.9	4.1	−3.5	P2q-T-31	313.7	3.3	−8.3
P2m-T-83	34.2	4.1	−6.0	P2m-T-32	156	4.2	−4.2	P2q-T-30	315.6	3.4	−8.1
P2m-T-82	36	4.1	−6.2	P2m-T-31	158	4.2	−4.8	P2q-T-29	316.1	2.8	−6.2
P2m-T-81	39.2	4.4	−6.8	P2m-T-30	160	4.5	−4.3	P2q-T-28	316.7	3.0	−5.5
P2m-T-80	43	4.4	−4.5	P2m-T-29	162	4.3	−3.8	P2q-T-27	317.2	3.0	−6.5
P2m-T-79	47	4.2	−4.8	P2m-T-28	164	4.0	−4.0	P2q-T-26	317.7	2.8	−6.5
P2m-T-78	52	4.3	−5.1	P2m-T-27	166	4.0	−4.8	P2q-T-25	318.1	2.7	−5.8
P2m-T-77	54.2	3.6	−4.1	P2m-T-26	168.2	4.5	−4.3	P2q-T-24	318.5	2.5	−5.6
P2m-T-76	60	2.0	−3.8	P2m-T-25	169	4.2	−3.5	P2q-T-23	318.9	3.0	−6.2
P2m-T-75	63	5.7	−5.4	P2m-T-24	170	4.2	−3.8	P2q-T-22	319.3	3.5	−8.0
P2m-T-74	64	3.1	−3.6	P2m-T-23	171	4.1	−4.2	P2q-T-21	320.2	3.2	−7.3
P2m-T-73	66	3.8	−7.3	P2m-T-22	173	4.0	−5.1	P2q-T-20	321	3.1	−7.2
P2m-T-72	67.3	4.0	−7.4	P2m-T-21	174.9	4.0	−3.7	P2q-T-19	321.9	2.8	−7.0
P2m-T-71	69	3.3	−2.4	P2m-T-20	179	3.7	−3.7	P2q-T-18	322.9	3.0	−6.6
P2m-T-70	71	3.0	−3.2	P2m-T-19	184	3.7	−3.7	P2q-T-17	324.9	3.3	−6.0
P2m-T-69	74	4.5	−2.8	P2m-T-18	188	4.0	−3.5	P2q-T-16	325.5	2.6	−6.3
P2m-T-68	77	4.0	−2.8	P2m-T-17	192	2.2	−5.7	P2q-T-15	327.9	2.9	−3.4
P2m-T-67	79.9	3.4	−4.4	P2m-T-16	196	1.8	−5.4	P2q-T-14	330.2	2.8	−7.1
P2m-T-66	81.9	5.2	−2.3	P2m-T-15	200	3.3	−5.0	P2q-T-13	331.2	2.5	−5.3
P2m-T-65	84.6	3.3	−5.3	P2m-T-14	203.3	2.5	−5.9	P2q-T-12	332.2	2.3	−3.3
P2m-T-64	85.4	5.2	−2.5	P2m-T-13	204.9	3.7	−3.8	P2q-T-11	333.2	2.4	−6.9
P2m-T-63	86	4.3	−4.6	P2m-T-12	206.2	3.8	−3.5	P2q-T-10	335.5	2.1	−6.9
P2m-T-62	87.2	3.8	−4.8	P2m-T-11	207.6	3.7	−3.5	P2q-T-9	337	2.2	−4.3
P2m-T-61	88.5	4.8	−4.3	P2m-T-10	209	3.7	−3.2	P2q-T-8	338.6	0.7	−5.2
P2m-T-60	89.5	4.0	−5.8	P2m-T-9	211	3.7	−2.9	P2q-T-7	339.1	−0.7	−4.5
P2m-T-59	91	4.2	−4.9	P2m-T-8	213	3.9	−2.9	P2q-T-6	339.9	1.2	−4.3
P2m-T-58	92.7	3.6	−6.0	P2m-T-7	215	3.9	−3.7	P2q-T-5	340.4	0.0	−4.7
P2m-T-57	94.7	4.1	−4.7	P2m-T-6	223	2.7	−5.4	P2q-T-4	340.9	1.5	−4.6
P2m-T-56	95.5	3.5	−4.7	P2m-T-5	232	2.9	−3.7	P2q-T-3	341.5	−0.4	−5.2
P2m-T-55	98	3.9	−4.8	P2m-T-4	239.4	3.9	−5.5	P2q-T-2	342.4	1.3	−6.7
P2m-T-54	101	3.4	−5.6	P2m-T-3	241.9	2.8	−2.9	P2q-T-1	343.7	−0.8	−6.9
P2m-T-53	104	3.9	−5.9	P2m-T-2	244.9	2.7	−3.4				
P2m-T-52	105.8	3.5	−6.9	P2m-T-1	245.3	2.0	−3.6				

time limit of a 3rd-order sequence. As a result, carbonate sedimentary filling rate is considered to be a constant factor in most cases, while GSL change and tectonic activity are the controlling factors of sedimentary sequences in marine carbonate rocks (Zhao et al., 2010). The depositional sequence in certain areas is controlled by relative changes in paleobathymetry resulted from GSL and/or tectonic activity.

Table 2
3rd-order sequence division of the middle Permian in the Sichuan Basin, China.

Series	Formation	Section	System domain	3rd-order sequence
Middle Permian	Maokou	Mao-4	HST	PSQ3
		Mao-3	TST	
		Mao-2	HST	PSQ2
		Mao-1	TST	
	Qixia	Qi-2	HST	PSQ1
		Qi-1	TST	
	Liangshan			

Extensive studies have indicated that C isotope of whole rock or fossil shell from marine carbonate rocks, such as brachiopods and other low-magnesium calcite shells, is indicative of relative GSL change, and the corresponding variations in O isotope ($\delta^{18}O$) reflect GSL change caused by glacier fluctuation (Sharp, 2007; Zhao et al., 2010; Grant, 2013). The C isotope value is generally positively correlated with GSL, while an increase in $\delta^{18}O$ content indicates the growth of glacier and fall of GSL (Williams, 1988; Feeley and Moore, 1990; Sharp, 2007). The thawing of glacier and the rise of sea level are favorable for preservation and bury of organic materials, leading to the loss of ^{12}C and relative enrichment of ^{13}C in crust surface hydrosphere, atmosphere and biosphere. However, it should be noted that ice can release ^{18}O into sea water and increase the $^{18}O/^{16}O$ ratio. The whole-rock C isotope values obtained from the Changjianggou outcrop in Guangyuan (Sichuan, China) show a low-

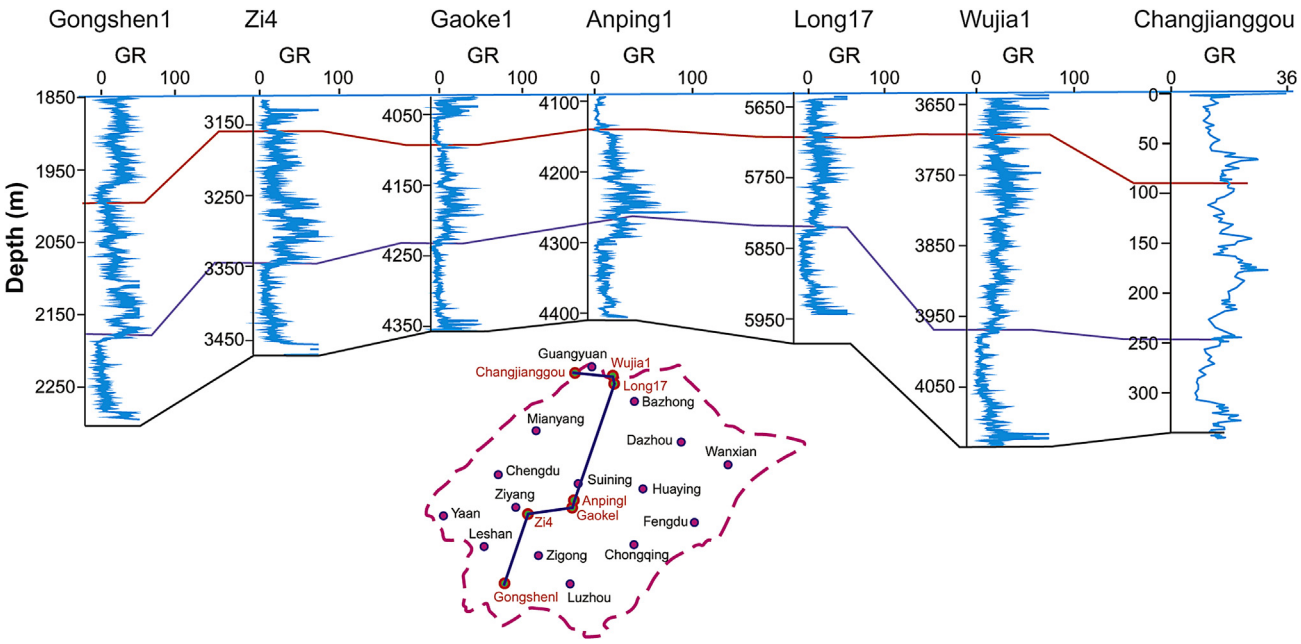

Figure 7. Drilling-outcrop cross section showing the sequence stratigraphic framework of the middle Permian in the Sichuan Basin (NS direction).

high-low trend, while the whole-rock O isotope values vary in an opposite trend. These results indicate that GSL has experienced a shallow-deep-shallow cycle, thus validating the proposed method for division of 3rd-order sequences.

As mentioned above, the changes in C and O isotopes reflect relative GSL changes, and detailed analysis of sedimentary facies shows relative changes in paleobathymetry of specific sedimentary sequence. Therefore, the similarity degree of these two changes can be used to infer the ancient tectonic subsidence-uplift during the deposition of the specific sedimentary sequence. If the variation trend in paleobathymetry is similar to that in GSL, i.e., the C and O isotope values show similar variation trends to paleobathymetry, the controlling factor of sedimentary sequence development will be GSL change, also known as GSL sequence. If the variation trend in paleobathymetry is completely deviated from the GSL variation trend and Milankovitch cycles recorded in strata are completely lost, regional tectonic subsidence, also known as tectonic sequence, is the controlling factor of the development of sedimentary sequence. Otherwise, the sedimentary sequence, i.e., tectonic-GSL composite sequence, is controlled by both GSL and tectonic movement. Although the trend in paleobathymetry deviates to some extent from the GSL trend, Milankovitch cycle still can be obtained from the frequency spectrum of stratigraphic record. To classify and identify 3rd-order sequence types is of great significance to geological research, and relevant study methods should be adjusted according to various controlling factors of 3rd-order sequence.

5.2. Sequence types and controlling factors

The whole-rock C isotope values of sequence PSQ1 show an increasing trend in the transgressive systems tract (Fig. 6), suggesting the elevation of GSL. There is a decreasing trend in the HST, suggesting the decline of GSL (Fig. 6). These findings indicate that the GSL variation trend reflected by the whole-rock C isotope curve has a high similarity with the relative paleobathymetric variation trend obtained via sedimentary subfacies analysis. Therefore, PSQ1 is considered to be a GSL sequence that is mainly controlled by GSL changes and features good global comparability. As for the condensed section of sequence PSQ2, the C isotope values are relatively low, suggesting the low level of GSL and consistent with the large paleobathymetry. Associated C isotope curve of the HST showed no substantial variation trend, mostly distributed in the range of large values and rarely in the range of small values. This observation indicates that GSL is overall high, consistent with the shallowing paleobathymetry of HST (Fig. 6). Similarly, the C isotope curve of sequence PSQ3 condensed section shows substantial variations and is clearly tooth-like, with no obvious elevation of GSL. In the HST, C isotopic values generally show an increasing trend, suggesting the high level of GSL. These indicate that there are substantial differences between the GSL relative variation trend indicated by the whole-rock C isotope curve and the relative paleobathymetry obtained via sedimentary subfacies analyses of sequences PSQ2 and PSQ3 (Fig. 6). Thus, the sequences PSQ2 and PSQ3 were affected by tectonic activity. Similarly, the O isotope values show an opposite variation trend to C isotope values. This validates the correctness of our method (Fig. 6).

The frequency spectra of natural gamma spectrum curve (Wu et al., 2012) were analyzed for the middle Permian sequences PSQ1–3 of well Long17 (Fig. 8). The results show that Milankovitch cycles recorded in the middle Permian strata of the Sichuan Basin are distinct (Fig. 8). Long (413.0 ka) and short (123.0 ka) eccentricity cycles are controlling factors for the development of high-frequency sequences in the early middle Permian strata in the basin, while long (413.0 ka) and short (123.0 and 95.0 ka) eccentricity cycles are the main factors of high-frequency sequence development in the Maokou Formation. Therefore, PSQ1 is a GSL sequence, whereas PSQ2 and PSQ3 are tectonic-GSL composite sequences.

This study suggests that, overall, the Sichuan Basin was a stable cratonic Mesa without substantial tectonic activity during the deposition of the Liangshan Formation and Qixia Formation. Therefore, the GSL sequence PSQ1 is established. We suggest that the Songpan-Ganzi ocean trough in the western basin started to have slow movement during the deposition of the Maokou Formation. This is different from previous explanation regarding the start of tectonic movement after the Maokou Formation and the development of siliceous nodules and bands over the basin. However, the Milankovitch data recorded in the Maokou Formation are

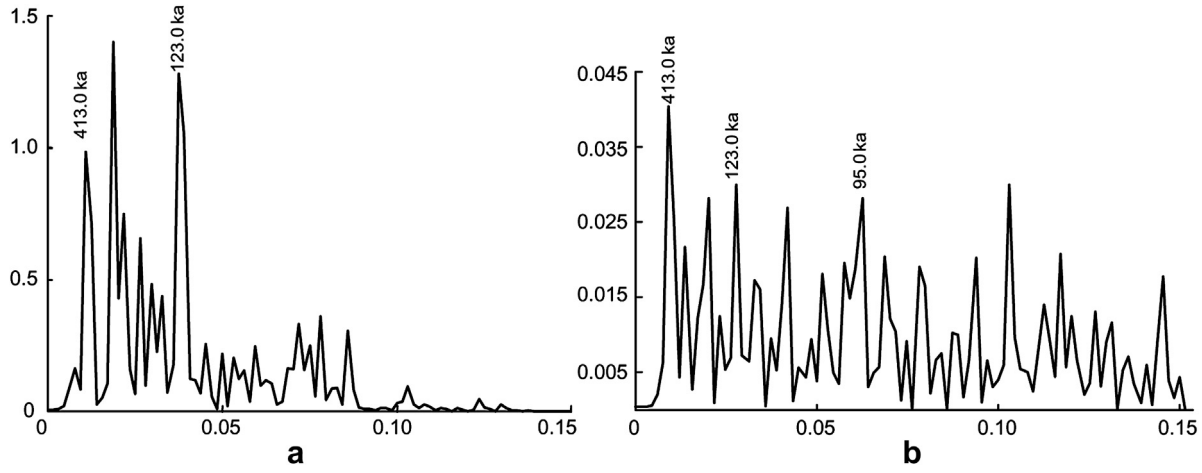

Figure 8. Frequency spectra of the natural gamma spectrum logging (ln(Th/K)) in the well Long17 in the Sichuan Basin, China. (a) Frequency spectra of PSQ1; (b) frequency spectra of PSQ2 and PSQ3.

still easily interpreted, showing a weak intensity of tectonic movement. Therefore, PSQ2 and PSQ3 are tectonic-GSL composite sequences controlled by tectonic activity and GSL change.

6. Conclusions

This study addresses the types and main controlling factors of 3rd-order sequences of the middle Permian strata in the Sichuan Basin, China. The conclusions are as follows:

(1) Through comprehensive analysis of C and O isotope trends, paleobathymetry and Milankovitch cycles, 3rd-order sequences can be divided into 3 types: (a) GSL sequence mainly controlled by GSL change, (b) tectonic sequence mainly controlled by regional tectonic activity, and (c) composite sequence jointly controlled by GSL change and regional tectonic activity.
(2) GSL sequences have global comparability while tectonic sequences have regional comparability. The spectra of certain logs for composite sequences show characteristics of Milankovitch cycles, thus featuring global comparability after filtering tectonic movement influence.
(3) The middle Permian strata developed three 3rd-order sequences, including PSQ1, PSQ2 and PSQ3 from bottom to top. PSQ1 is a GSL sequence while PSQ2 and PSQ3 are composite sequences. These indicate that the depositional environment was stable during the depositional period of PSQ1, but was activated by tectonic activity during the deposition of the middle Permian Maokou Formation.

The classification of 3rd-order sequences and identification of their main controlling factors form the foundation for division of high-frequency sequences, precise stratigraphic correlation, and analysis of sedimentary environment change are of great theoretical value and practical significance to relevant geological researches.

Acknowledgments

Our research was part of a key project carried out in 2008–2011 and was financially supported by the National Major Special Science and Technology Project (Grant No. 2008ZX05004-001) and a Major Special Issue of the China National Petroleum Corporation (Grant No. 2008E-0702). The authors are grateful to the reviewers and GSF editors for critical evaluation of the manuscript and valuable suggestions leading to substantial improvements.

References

Abbott, S.T., Sweet, I.P., 2000. Tectonic control on third-order sequences in a siliciclastic ramp-style basin; an example from the Roper Superbasin (Mesoproterozoic), northern Australia. Australian Journal of Earth Sciences 47 (3), 637–657.
Cathles, L.M., Hallam, A., 1991. Stress-induced changes in plate density, Vail sequences, epeirogeny, and short-lived global sea level fluctuations. Tectonics 10 (4), 659–671.
Chen, Z.Q., Huang, Y.L., Zhang, X.M., Liu, F.C., 2007. Sedimentary Characteristics of the Formations of Maokou and Qixia in the Middle Permian, the Sichuan Basin. Internal Report (in Chinese).
Duncan, D.S., Hine, A.C., Droxler, A.W., 1999. Tectonic controls on carbonate sequence formation in an active strike-slip setting; Serranilla Basin, northern Nicaragua Rise. Marine Geology 160 (3–4), 355–382.
Feeley, M.H., Moore, T.C., Loutit, T.S., Bryant, W.R., 1990. Sequence stratigraphy of Mississippi Fan related to oxygen isotope sea level index [J]. AAPG Bulletin 74, 407–424.
Grant, M.Y., 2013. Precambrian supercontinents, glaciations, atmospheric oxygenation, metazoan evolution and an impact that may have changed the second half of Earth history. Geoscience Frontiers 4, 247–261.
Haq, B.U., Schutter, S.R., 2008. A chronology of Paleozoic sea-level changes. Science 322 (5898), 64–68.
Haq, B.U., Hardenbol, J., Vail, P.R., 1987. Chronology of fluctuating sea levels since the Triassic. Science 235 (4793), 1156–1167.
Horton, B.K., Constenius, K.N., DeCelles, P.G., 2004. Tectonic control on coarse-grained foreland-basin sequences: an example from the Cordilleran foreland basin. Utah Geology 32, 637–640.
Lazauskiene, J., Sliaupa, S., Brazauskas, A., Musteikis, P., 2003. Sequence stratigraphy of the Baltic Silurian succession; tectonic control on the foreland infill. In: McCann, T., et al. (Eds.), Tracing Tectonic Deformation Using the Sediment Record. Geological Society Special Publications, vol. 208, pp. 23–43.
Li, F.J., Chen, S.R., 2008. Study on the middle-lower Permian sequence stratigraphy in Northeastern area, the Sichuan Basin. Petroleum Geology and Experiment 30 (5), 472–477 (in Chinese with English abstract).
Ma, Y.S., Mei, M.X., Chen, X.B., Wang, G.W., Zhou, L., 1999. Carbonate Reservoir Sedimentology. Part 2. Geological Publishing House, Beijing, pp. 104–155 (in Chinese).
Macdonald, D.I.M. (Ed.), 1991. Sedimentation, Tectonics and Eustasy: Sea-level Changes at Active Margins. International Association of Sedimentologists Special Publication, vol. 12, p. 518.
Miall, A.D., 1994. Sequence stratigraphy and chronostratigraphy; problems of definition and precision in correlation, and their implications for global eustasy. Geoscience Canada 21 (1), 1–26.
Miall, A.D., 2000. Principles of Sedimentary Basin Analysis. Springer, Berlin, Federal Republic of Germany, Berlin, pp. 1–616.
Plint, A.G., Eyles, N., Eyles, C.H., Walker, R.G., 1992. Control of sea level change. In: Walker, R.G., James, N.P. (Eds.), Facies Models; Response to Sea Level Change. Geological Association of Canada, St. Johns, NL, Canada, pp. 15–25.
Qin, J.X., Zeng, Y.F., Chen, H.D., Tian, J.C., Li, Y.S., Qian, Y.Z., Shou, J.F., Shen, A.J., 1999. Permian sequence stratigraphy and sea-level changes in southwestern China. Journal of Lithofacies Paleogeography 18 (1), 19–34 (in Chinese).

Sabadini, R., Doglioni, C., Yuen, D.A., 1990. Eustatic sea level fluctuations induced by polar wander. Nature 345 (6277), 708–710.
Sarg, J.F., 1988. Carbonate sequence stratigraphy. In: Wilgus, C.K., et al. (Eds.), Sea Level Changes – an Integrated Approach. SEPM Special Publication No. 42, pp. 155–181.
Schlager, W., 2005. Carbonate Sedimentology and Sequence Stratigraphy. SEPM Special Publication – Concepts in Sedimentology and Paleontology No. 8, pp. 1–198.
Sharp, Z., 2007. Principles of Stable Isotope Geochemistry. Pearson Education, U.S.A., Houston, p. 380.
Tucker, M.E., Wright, V.P., Dickson, J.A.D., 1990. Carbonate Sedimentology. Blackwell Sci. Publ., Oxford, United Kingdom, London, pp. 1–482.
Vail, P.R., Audemard, F., Bowman, S.A., Eisner, P.N., Perez-Cruz, G., 1991. The stratigraphic signatures of tectonics, eustacy and sedimentology; an overview. In: Einsele, G., et al. (Eds.), Cycles and Events in Stratigraphy. Springer Verlag, Berlin, Berlin, pp. 617–659.
Wang, C.S., Chen, H.D., Shou, J.F., Li, X.H., Tian, J.C., Qin, J.X., 1999. Characteristics and correlation of Permian depositional sequences in South China. Acta Sedimentologica Sinica 17 (4), 499–509 (in Chinese).
Ward, W.B., 1999. Tectonic control on backstepping sequences revealed by mapping of Frasnian backstepped platforms, Devonian reef complexes, Napier Range, Canning Basin, Western Australia. In: Harris, P.M., et al. (Eds.), Advances in Carbonate Sequence Stratigraphy; Application to Reservoirs, Outcrops and Models, Special Publication-Society for Sedimentary Geology, 63, pp. 47–74.
Wilson, J.L., 1975. Carbonate Facies in Geologic History. Springer, New York, pp. 1–471.
Williams, D.F., 1988. Evidence for and against sea-level changes from the stable isotopic record of the Cenozoic [A]. In: Wilgus, C.K. (Ed.), Sea-level Changes; An Integrated Approach [C], Special Publication – Society of Economic Paleontologists and Mineralogists 42, pp. 31–36.
Wu, L., Li, F., Zhu, C., Li, L., 2012. Holocene environmental change and archaeology, Yangtze River valley, China: Review and prospects. Geoscience Frontiers 3 (6), 875–892.
Wu, L.Q., Hu, M.Y., Hu, Z.G., Xiang, J., 2010. Study on the middle Permian sequence stratigraphy of Sichuan Basin. Petroleum Geology and Engineering 24 (6), 10–13 (in Chinese with English abstract).
Xu, S.L., Chen, H.D., Chen, A.Q., Lin, L.B., Li, J.W., Yang, J.B., Gao, S., 2011. Distribution of source-reservoir-cap rock assemblages within the sequence framework from the Devonian to the Middle Triassic in the Sichuan Basin. Petroleum Exploration and Development 38 (2), 159–167 (in Chinese with English abstract).
Zhang, Y.B., Zhao, Z.J., Yuan, S.Q., Zheng, M., 2011. Application of spectral analysis to identify Milankovitch cycles and high-frequency sequences. Journal of Jilin University (Earth Science Edition) 41 (2), 400–410 (in Chinese with English abstract).
Zhao, Z.J., Chen, X., Pan, M., Wu, X.N., Zheng, X.P., Pan, W.Q., 2010. Cambrian sequence stratigraphic framework in Tarim Basin. Acta Geologica Sinica 84 (4), 518–536 (in Chinese with English abstract).
Zhou, Y., Chen, H.D., Wang, C.S., Jin, Z.J., Tang, L.J., Wang, Z.Y., Liang, X.W., 2005. The Middle Permian sequence stratigraphy of the Mid-Yangze area. Journal of Stratigraphy 29 (3), 270–280 (in Chinese with English abstract).